Inorg. Chem. **2007**, *46*, 9221–9233

Nickel–Cysteine Binding Supported by Phosphine Chelates

Patrick J. Desrochers,*,† Davis S. Duong,† Ariel S. Marshall,† Stacey A. Lelievre,† Bonnie Hong,† Josh R. Brown,† Richard M. Tarkka,† Jerald M. Manion,† Garen Holman,† Jon W. Merkert,‡ and David A. Vicic§,||

Department of Chemistry, University of Central Arkansas, Conway, Arkansas 72035, Department of Chemistry, The University of North Carolina at Charlotte, Charlotte, North Carolina 28223, and Department of Chemistry and Biochemistry, University of Arkansas, Fayetteville, Arkansas 72701

Received June 12, 2007

The effect of chelating phosphines was tested on the structure and pH-dependent stability of nickel–cysteine binding. (1,2-Bis(diphenylphosphino)ethane (dppe) and 1,1,1-tris[(diphenylphosphino)methyl]ethane (triphos) were used with three different cysteine derivatives (L-cysteine, Cys; L-cysteine ethyl ester, CysEt; cystamine, CysAm) to prepare complexes of the form (dppe)NiCysR^{n+} and (triphos)NiCysR^{n+} ($n = 0$ for Cys; $n = 1$ for CysEt and CysAm). Similar ^{31}P $\{^1$H$\}$ NMR spectra for all (dppe)NiCysR^{n+} confirmed their square-planar P_2NiSN coordination spheres. The structure of [(dppe)NiCysAm]PF_6 was also confirmed by single-crystal X-ray diffraction methods. The (triphos)-NiCysAm$^+$ and (triphos)NiCysEt$^+$ complexes were fluxional at room temperature by ^{31}P NMR. Upon cooling to –80 °C, all gave spectra consistent with a P_2NiSN coordination sphere with the third phosphorus uncoordinated. Temperature-dependent ^{31}P NMR spectra showed that a trans P–Ni–S π interaction controlled the scrambling of the coordinated triphos. In aqueous media, (dppe)NiCys was protonated at pH $\sim$ 4–5, leading to possible formation of a nickel–cysteinethiol and eventual cysteine loss at pH < 3. The importance of N-terminus cysteine in such complexes was demonstrated by preparing (dppe)NiCys-bead and trigonal-bipyramidal Tp*NiCys-bead complexes, where Cys-bead represents cysteine anchored to polystyrene synthesis beads and Tp*$^-$ = hydrotris(3,5-dimethylpyrazolyl)borate. Importantly, results with these heterogeneous systems demonstrated the selectivity of these nickel centers for cysteine over methionine and serine and most specifically for N-terminus cysteine. The role of Ni–S π bonding in nickel–cysteine geometries will be discussed, including how these results suggest a mechanism for the movement of electron density from nickel onto the backbone of coordinated cysteine.

Introduction

Complexes of nickel, hydrogen, and sulfur play a role in important industrial and biochemical processes. The direct coordination of one or more sulfur atoms to nickel is found in the majority of redox-active bacterial nickel enzymes, and in most cases, this sulfur is provided by cysteine.[1] Examples include [NiFe] hydrogenases,[2] carbon monoxide dehydrogenase,[3] acetyl−coenzyme A (CoA) synthase,[4] and a special class of superoxide dismutases that utilize nickel (NiSOD).[5] Notable exceptions without direct nickel−cysteine coordination include acireductone dioxygenase[6] and methyl−

* To whom correspondence should be addressed. E-mail: patrickd@uca.edu.
† University of Central Arkansas.
‡ The University of North Carolina at Charlotte.
§ University of Arkansas.
|| Current address: Department of Chemistry, University of Hawaii, 2545 McCarthy Mall, Honolulu, HI, 96822.

(1) (a) Thauer, R. K. *Science*, **2001**, *293*, 1264−1265. (b) *Transition Metal Sulfur Chemistry: Biological and Industrial*; Steifel, E. I., Matsumoto, K., Eds.; ACS Symposium Series 653; American Chemical Society: Washington, DC, 1996; Chapter 4.
(2) (a) Volbeda, A.; Garcin, E.; Piras, C.; de Lacey, A. L.; Fernandez, V. M.; Hatchikian, E. C.; Frey, M.; Fontecilla-Camps, J. C. *J. Am. Chem. Soc.* **1996**, *118*, 12989−12996. (b) Gu, Z.; Dong, J.; Allan, C. B.; Choudhury, S. B.; Franco, R.; Moura, J. J. G.; Moura, I.; LeGall, J.; Przybyla, A. E.; Roseboom, W.; Albracht, S. P. J.; Axley, M. J.; Scott, R. A.; Maroney, M. J. *J. Am. Chem. Soc.* **1996**, *118*, 11155−11165.
(3) (a) Dobbek, H.; Svetlitchnyi, V.; Gremer, L.; Huber, R.; Meyer, O. *Science*, **2001**, *293*, 1281−1285. (b) Feng, J.; Lindahl, P. A. *J. Am. Chem. Soc.* **2004**, *126*, 9094−9100.
(4) (a) Tan, X.; Surovtsev, I. V.; Lindahl, P. A. *J. Am. Chem. Soc.* **2006**, *128*, 12331−12338. (b) Tan, X.; Loke, H.-K.; Fitch, S.; Lindahl, P. A. *J. Am. Chem. Soc.* **2005**, *127*, 5833−5839.
(5) Barondeau, D. P.; Kassmann, C. J.; Bruns, C. K.; Tainer, J. A.; Getzoff, E. D. *Biochemistry* **2004**, *43*, 8038−8047.
(6) Szajna, E.; Dobrowolski, P.; Fuller, A. L.; Arif, A. M.; Berreau, L. M. *Inorg. Chem.* **2004**, *43*, 3988−3997.

10.1021/ic701150q CCC: $37.00
Published on Web 09/14/2007

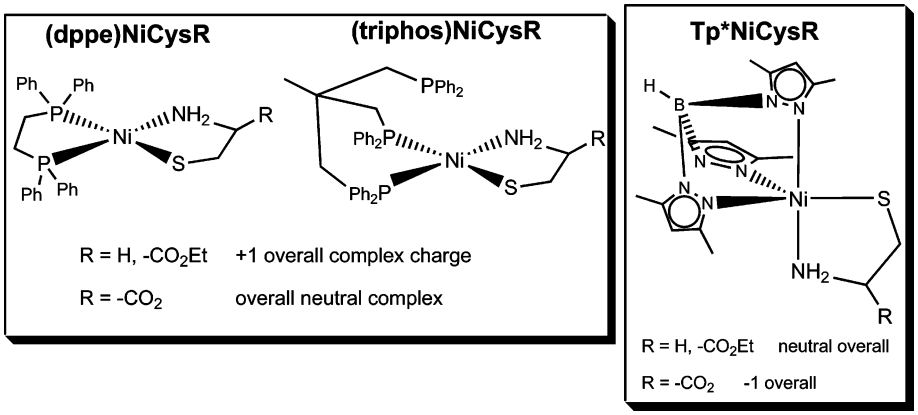

Figure 1. Nickel−cysteine coordination geometries resulting from different phosphorus- and nitrogen-donor chelates. Charges on the resulting complexes vary from 1+, to 0, to 1−, depending on the ligand (dppe, triphos, or Tp*$^-$) and cysteine derivative (Cys^{2-}, CysEt$^-$, or CysAm$^-$) charges.

coenzyme M reductase (MCR), although MCR does involve methyl thioether/thiyl radical association with nickel.[7] Such enzymes catalyze reactions that parallel commercially valuable processes including hydrogen consumption ([NiFe] hydrogenases), hydrogen production via the water−gas shift reaction (CODH), and the generation of methane from biomass (CODH and MCR). Nickel−cysteine systems that model characteristics of these enzymes remain a persistent area of fruitful research.

Recent work by Riordan's[8] and Darensbourg's[9] groups has explored the coordination of nickel with chelating cysteine and phosphines. Both groups reported square-planar complexes of nickel using the tripeptide Cys−Gly−Cys, leading to NiN_2S_2 coordination spheres reminiscent of the distal nickel site in acetyl−CoA synthase. In separate experiments, they demonstrated the ability of *cis*-NiN_2S_2 groups to chelate via bridging thiolates to secondary metals including Ni(dppe) [where dppe = 1,2-bis(diphenylphosphino)ethane],[8] $W(CO)_4$,[9] $Rh(CO)_2$,[9] and $Pd(Cl)(CH_3)$.[9] These results reinforced the belief that the distal nickel site in acetyl−CoA synthase is part of a supporting ligand for the proximal nickel center where active acetyl synthesis takes place.[10] Darensbourg's group anchored this Cys−Gly−Cys peptide to a heterogeneous support and showed that its chelation of nickel(II) was unaltered.[9]

Square-planar nickel−cysteine coordination spheres are the norm in synthetic complexes;[11] however, ancillary ligands can alter this geometric pattern. Thermally stable five-coordinate nickel−cysteine geometries resulted when tridentate tris(pyrazolyl)borate chelates (i.e., Tp*$^-$, hydrotris-(3,5-dimethylpyrazolyl)borate; Figure 1) were used.[12] Nickel(II) ligated by Tp*$^-$ selectively bound cysteine and selenocysteine, producing analogous static five-coordinate geometries.[12,13] In contrast, the present results with triphos [a *fac*-P_3 donor; 1,1,1-tris[(diphenylphosphino)methyl]ethane] show fluxional systems that exchange between four-coordinate P_2-NiSN and transient five-coordinate P_3NiSN coordination spheres. The Tp*Ni^+ Lewis acid center also discriminated between cysteine and homocysteine and the methyl thioether of cysteine.[13]

Throughout all of the cysteine work to date, nickel−cysteine*thiol* remains an elusive synthetic goal. Interest in nickel−cysteine protonation stems from its invocation in proposed catalytic cycles of [NiFe]Hase[14] and NiSOD enzymes,[15] where it may also be coupled with electron transport. Nickel−cysteine protonation coupled with electron transport has been implicated in catalytic hydrogen generation in aqueous media.[16] Work by Henderson's group has demonstrated that coordinated phosphines level the acidities of Ni−SR groups (R = Et and a variety of phenyls).[17] Possible proton sharing between nickel and sulfur was suggested in these systems, facilitated by phosphine backbonding that draws thiolate electron density onto nickel.[17]

The present work describes the effect of triphos on nickel−cysteine geometries and the pH stability of cysteine coordinated to (dppe)Ni^{2+}. Considerable differences in coordination geometries between nickel and cysteine result when triphos replaces Tp*$^-$. Square-planar diamagnetic nickel−cysteine complexes were not observed with tridentate Tp*$^-$,[12,13] but these are described here for triphos. Experi-

(7) (a) Craft, J. L.; Horng, Y.-C.; Ragsdale, S. W.; Brunold, T. C. *J. Am. Chem. Soc.* **2004**, *126*, 4068−4069. (b) Ermler, U.; Grabarse, W.; Shima, S.; Goubeaud, M.; Thauer, R. K. *Science* **1997**, *278*, 1457−1462.
(8) Krishnan, R.; Riordan, C. G. *J. Am. Chem. Soc.* **2004**, *126*, 4484−4485.
(9) Green, K. N.; Jeffery, S. P.; Reibenspies, J. H.; Darensbourg, M. Y. *J. Am. Chem. Soc.* **2006**, *128*, 6493−6498.
(10) Webster, C. E.; Darensbourg, M. Y.; Lindahl, P. A.; Hall, M. B. *J. Am. Chem. Soc.* **2004**, *126*, 3410−3411.
(11) (a) Nivorozhkin, A. L.; Segal, B. M.; Musgrave, K. B.; Kates, S. A.; Hedman, B.; Hodgon, K. O.; Holm, R. H. *Inorg. Chem.* **2000**, *39*, 2306−2313. (b) Baidya, N.; Ndreu, D.; Olmstead, M. M.; Mascharak, P. K. *Inorg. Chem.* **1991**, *30*, 2448−2451. (c) Kozlowski, H.; Decock-Le Révérend, B.; Ficheux, D.; Loucheux, C.; Sovago, I. *J. Inorg. Biochem.* **1987**, *29*, 187−197.
(12) Desrochers, P. J.; Cutts, R. W.; Rice, P. K.; Golden, M. L.; Graham, J. B.; Barclay, T. M.; Cordes, A. W. *Inorg. Chem.* **1999**, *38*, 5690−5694.
(13) Desrochers, P. J.; Abrams, M.; Nutt, D.; Arvin, M. E.; Phelps, A. L. 20th International Conference on the Organic Chemistry of Sulfur, Northern Arizona University, Flagstaff, AZ, July 2002.
(14) (a) Fan, H.-J.; Hall, M. B. *J. Am. Chem. Soc.* **2002**, *124*, 394−395. (b) Stadler, C.; de Lacey, A. L.; Montet, Y.; Volbeda, A.; Fontecilla-Camps, J. C.; Conesa, J. C.; Fernández, V. M. *Inorg. Chem.* **2002**, *41*, 4424−4434.
(15) Pelmenschikov, V.; Siegbahn, P. E. M. *J. Am. Chem. Soc.* **2006**, *128*, 7466−7475.
(16) (a) Bănică, F. G. *Bull. Soc. Chim. Fr.* **1991**, *128*, 697−703. (b) Bănică, F. G.; Diacu, E. *Collect. Czech., Chem. Commun.* **1991**, *56*, 140−151.
(17) Clegg, W.; Henderson, R. A. *Inorg. Chem.* **2002**, *41*, 1128−1135.

mental verification for the importance of π bonding between triphos and the nickel−cysteine group is presented as a driving force in this geometric variation. A limit on the pH-dependent stability of nickel−cysteine chelation was determined for (dppe)NiCys.

Amino acids and short cysteine−peptides anchored to polystyrene synthesis beads were also tested against Tp^*Ni^+ and $(dppe)Ni^{2+}$ to determine the effect of Tp^{*-} and dppe on the selectivity of nickel for cysteine and related residues. The spectroscopic results presented here confirm the geometry of the heterogeneous products and demonstrate that the heterogeneous systems are identical with their homogeneous small-molecule counterparts.

Experimental Section

Spectroscopy. Room-temperature Fourier transform (FT) NMR spectra were recorded using a JEOL ECX 300 MHz spectrophotometer. This spectrometer is equipped with a variable-temperature attachment. FTIR spectra were recorded for samples pressed as KBr pellets using a Thermo Nicolet IR 100 spectrometer at ambient temperature. UV−vis electronic spectra were recorded at room temperature using a Cary 50 spectrometer and 1 cm path length quartz cuvettes.

Mass Spectrometry. Spectra were recorded using a PE Biosystem Mariner electrospray ionization time-of-flight mass spectrometer. The sample was introduced via a direct-infusion syringe pump (10 μL/min). Nozzle and skimmer voltages were optimized to prevent fragmentation and solvent clustering. The nozzle was held at a temperature of 125 °C. Prior to recording sample spectra, the instrument was calibrated with Perceptive Biosystems Cal Mix (containing bradykinin, angiotensin, and neutrotensin).

Synthesis of Nickel Complexes. All reagents, ligands, and precursor complexes, $(dppe)NiCl_2$, were obtained from Sigma-Aldrich, unless otherwise noted. All solvents were obtained from Fisher Scientific and used as received. The primary syntheses for all of the $(dppe)NiCysR^{n+}$ products were carried out under an inert nitrogen atmosphere to retard oxidation of thiolate anion intermediates. Final workup and purification were performed open to the air. All $(triphos)NiCysR^+$ preparations and manipulations were carried out under a constant nitrogen atmosphere to reduce oxidation of the pendant uncoordinated phosphine. Elemental analyses were performed by Atlantic Microlab, Norcross, GA.

Synthesis and Purification of [(dppe)NiCysEt]Cl. A solution of L-cysteine ethyl ester hydrochloride (71 mg, 0.38 mmol) was prepared in 5 mL of degassed methanol, and 2.4 mol equiv of degassed triethylamine (93 mg, 0.91 mmol) was added to deprotonate the amino acid ethyl ester in situ. This cysteine thiolate solution was transferred via a cannula needle to a dark-orange slurry of $(dppe)NiCl_2$ (200 mg, 0.38 mmol) in 60 mL of methanol. The mixture was stirred for an additional 30 min, affecting complete dissolution of $(dppe)NiCl_2$, and then stripped to dryness. Diethyl ether added to the resultant residue induced the formation of a microcrystalline solid. This solid was purified using column chromatography: column dimensions = 3 cm × 8 cm using 70−270 mesh, 60 Å silica gel stationary phase (Aldrich); chloroform/methanol mobile phase. For the first 2 h, a 90:10 chloroform/methanol eluent was used. This was changed to an 80:20 mixture for the final 2−3 h of separation. Leading bands were identified as (dppe)O (^{31}P NMR in $CDCl_3$: −11.3 and 33.4 ppm) and occasionally unreacted $(dppe)NiCl_2$ (^{31}P NMR: 58.2 ppm). The more polar product eluted last as a dark-orange band. Yield: 150 mg. Anal. Expt (theory): C, 56.23 (58.10); H, 5.56 (5.35); N, 2.20 (2.19). ^{13}C {^{1}H} NMR ($CDCl_3$): δ 171.9 (−C(=O)−), 135−127 (Ph), 64.1 (d, C_α, J_{CP} = 9.1 Hz), 61.7 (−C(O)CH_2−), 33.9 (d, C_β, J_{CP} = 11.3 Hz), 27.7 (d/d, −PCH_2−, J_{CP} = 16.0 and 31.9 Hz), 25.4 (d/d, −PCH_2−, J_{CP} = 11.8 and 32.6 Hz), 14.0 (−C(O)CH_2CH_3). ^{31}P NMR (Table 3). UV−vis ($CHCl_3$): 382 nm (ϵ = 1110 M^{-1} cm^{-1}), 492 sh (ϵ = 180).

Preparation of (dppe)NiCys. A total of 400 mg (0.76 mmol) of $(dppe)NiCl_2$ and 92 mg (0.76 mmol) of L-cysteine were placed into separate Schlenk flasks under nitrogen. A total of 80 mL of degassed methanol was added to $(dppe)NiCl_2$, creating a red-orange slurry. Degassed triethylamine (0.5 mL) was added to cysteine dissolved in 10 mL of degassed methanol. This solution was stirred vigorously and then transferred via a cannula needle to the flask containing the $(dppe)NiCl_2$/methanol mixture. A slight color change from dark orange to light orange was observed after the cysteine was added. The solution was allowed to stir for approximately 30 min, completing the dissolution and reaction of $(dppe)NiCl_2$, and then concentrated to a dark-orange syrup under nitrogen. Diethyl ether was added to this residue to precipitate the light-orange material. The solid was purified by column chromatography (70:30 chloroform/methanol mobile phase, 3 cm × 18 cm column made from 70−270 mesh, 60 Å silica gel as the stationary phase). The solid extracted from the eluted residue was washed repeatedly with diethyl ether to remove residual methanol. Yield: 200 mg. MS (0.1% acetic acid/acetonitrile): *m*/*z* 576, $(dppe)Ni(Cys)H^+$. IR (KBr): 1102 cm^{-1} (m, C−N), 1450 (s), 1600 (s, R−CO_2), 3045 (m, C=C−H), 3300 (w, R−NH_2). ^{31}P NMR: see Table 3. UV−vis (CH_3OH): 381 nm (ϵ = 730 M^{-1} cm^{-1}), 495 sh (ϵ = 90).

Preparation of [(dppe)NiCysAm]PF_6. This synthesis was carried out following the same method as that of (dppe)NiCys using 2-aminoethanethiol hydrochloride (86 mg, 0.76 mmol). A concentrated solution of ammonium hexafluorophosphate (370 mg in 0.5 mL of deionized water) was added, the mixture was cooled in an ice bath, and an additional 20 mL of deionized water was added to induce precipitation of the product as a light-orange solid. The solid was filtered and washed with deionized water and cold isopropyl alcohol. Yield: 390 mg. Anal. Expt (theory): C, 49.60 (49.51); H, 4.47 (4.48); N, 2.07 (2.08). IR (KBr): 839 cm^{-1} (vs, PF_6^-), 1103 (m, C−N), 1436 (m), 3259 (m, R−NH_2). ^{31}P NMR: see Table 3. UV−vis (CH_3OH): 379 nm (ϵ = 810 M^{-1} cm^{-1}), 494 sh (ϵ = 90).

Preparation of [(triphos)NiCysAm]PF_6. The precursor complex $(triphos)NiCl_2$ was prepared, isolated under nitrogen, and then used immediately to form the cysteine adducts. $(Triphos)NiCl_2$ was prepared according to literature methods[18] using 200 mg (0.32 mmol) of triphos and 76 mg (0.32 mmol) of $NiCl_2 \cdot 6H_2O$. This precursor was isolated upon removal of the reaction solvent under nitrogen. Degassed methanol (15 mL) was added to the bright-orange $(triphos)NiCl_2$, giving a slurry of a green solution [solvated $(triphos)NiCl_2$] and an undissolved orange solid. In a separate Schlenk flask was prepared a solution of 2-aminoethanethiol hydrochloride (36 mg, 0.32 mmol) in 3 mL of methanol, and to this solution was added 0.10 mL of degassed triethylamine. The deprotonated aminoethanethiol/methanol solution was transferred via a cannula needle to the $(triphos)NiCl_2$/methanol mixture, leading to a color change to light orange and the dissolution of all solids after stirring for about 30 min. To this mixture was added a degassed concentrated aqueous ammonium hexafluorophosphate solution (630 mg in 2 mL), inducing immediate precipitation of the product

(18) Kandiah, M.; McGrady, G. S.; Decken, A.; Sirsch, P. *Inorg. Chem.* **2005**, *44*, 8650−8652.

as a pale-orange solid. The product was washed with deionized water and dried in vacuo under nitrogen. Yield: 250 mg. Anal. Expt (theory): C, 59.92 (61.03); H, 5.44 (5.36); N, 1.66 (1.66). IR (KBr): 838 (vs, PF_6^-), 1097 (s, C−N), 1435 (s), 3250 (m, R−NH_2). ^{31}P NMR: see Table 3.

Preparation of [(triphos)NiCysEt]PF_6. This synthesis was carried out by the same method as that for [(triphos)NiCysAm]-PF_6 using 59 mg (0.32 mmol) L-cysteine ethyl ester hydrochloride. The product was isolated as a light-orange solid. Yield: 260 mg. Anal. Expt (theory): C, 56.75 (56.58); H, 5.13 (5.06); N, 1.46 (1.43). IR (KBr): 840 (vs, PF_6), 1435 (s), 1735 (s, ester), 3248 and 3304 (R−NH_2). ^{31}P NMR: see Table 3.

Preparation of [(dppe)NiSeCysAm]Cl in Situ. A degassed solution of methanol was added to a septum-fitted, purged bottle containing 30 mg of selenocystamine dihydrochloride. This material was purchased from ICN Biomedicals as a yellow diselenide. A methanolic slurry of sodium borohydride was titrated into the yellow diselenide solution until it was colorless, indicating complete reduction to 2 equiv of the alkylselenide anion. This alkylselenide solution was transferred to a waiting 50 mg sample of air-free (dppe)$NiCl_2$ in methanol using a gastight syringe. A slight immediate color change was observed. The orange supernatant was loaded into a septum-fitted NMR tube under nitrogen, and the ^{31}P {^{1}H} NMR spectrum was recorded as it was for the other samples. NMR results are summarized in Table 3.

Synthesis of Bead-Supported Peptides. Argogel−NH_2 polystyrene synthesis beads, with a functional group density of 0.40 mmol of −NH_2 per 1 g of beads, were obtained from Aldrich. They were thoroughly washed and swollen with a 50:50 mixture of *N*,*N*-dimethylformamide (DMF)/CH_2Cl_2 prior to use. All other reagents used in the synthesis of the oligopeptides on beads were used as received. Fmoc-protected amino acids were obtained from Nova-Biochem (EMD Biosciences). Piperidine, hydroxybenzotriazole (HOBt), trifluoroacetic acid, diisopropylsilane, and diisopropylcarbodiimide (DIPCDI) were obtained from Aldrich. Kaiser test reagents were obtained as a kit from Fluka.

Fmoc-protected amino acids were added to the synthesis beads using the standard OBt ester formation protocol as described in the 2006/2007 Novabiochem (EMD Biosciences) catalog, p 3.2. Representative synthesis: 595 mg (2.0 mmol, 5-fold excess) of Fmoc-protected glycine and 270 mg (2.0 mmol, 5-fold excess) of HOBt were dissolved in 20 mL of a 50:50 mixture of DMF/CH_2Cl_2, after which DIPCDI (250 mg, 2.0 mmol, 5-fold excess) was added. The mixture was stirred for about 10 min. The mixture was added to 1.0 g of washed and swollen Argogel beads. The slurry was rotated for several hours. Completeness of the addition of the amino acid to the beads was tested using a standard Kaiser test as described on p 3.4 of the 2006/2007 Novabiochem (EMD Biosciences) catalog. The Fmoc protecting groups were removed by rotating the beads for 30 min with 20 mL of a 20:80 mixture of piperidine/DMF. This was done several times, after which the beads were given a final wash with DMF. Removal of the Fmoc group was confirmed with a Kaiser test. The trityl protecting group on the cysteine residues and the *tert*-butyl protecting groups on serine were both removed with a 95:5 mixture of trifluoroacetic acid/triisopropylsilane.

Reaction of (dppe)$NiCl_2$ and Tp*$NiNO_3$ with Bead-Bound Peptides (AA_n-bead). Tp*$NiNO_3$ used in these experiments was prepared according to literature methods.[12,19] Separate methanolic solutions of the two nickel precursors (10−15 mg of each in 2 mL) were prepared under nitrogen, and degassed triethylamine (25 μL) was added to each in order to deprotonate cysteinethiols when introduced to AA_n-bead. Samples of AA_n-bead were loaded into septum-fitted vials and purged with nitrogen. The nickel-complex solutions were added to each of the AA_n-bead samples using a gastight syringe. Reaction was noted by pronounced color changes, indicative of the formation of green Tp*NiCys−AA_n-bead and orange (dppe)NiCys−AA_n-bead whenever Cys was located at the N-terminus site of the peptide sequence. These results are illustrated in Figure 7.

In order to obtain spectroscopic confirmation for the bead-bound product, a sample of (dppe)NiCys-bead was prepared in chloroform following the procedure described above but with the Cys-beads in a nitrogen-purged, septum-fitted NMR tube. A solution of (dppe)-$NiCl_2$ (10 mg and 50 μL of degassed triethylamine) in 0.6 mL of degassed $CDCl_3$ was prepared under a nitrogen atmosphere. The originally colorless beads immediately became bright-orange when (dppe)$NiCl_2$ was added. Although the (dppe)NiCys-bead product floated at the top of the reaction mixture, spinning while recording the ^{31}P NMR spectrum sufficiently homogenized the mixture, adequate lock and shim was obtained, and a ^{31}P {^{1}H} NMR spectrum was recorded on this slurry (Figure 8). The supernatant containing unreacted (dppe)$NiCl_2$ was removed, and the beads were washed several times with fresh chloroform using a syringe through the septum fitting. The bright-orange beads were resuspended in fresh chloroform, and the spectrum of just the suspended (dppe)-NiCys-bead product was recorded (Table 3 and Figure 8).

pH-Dependent ^{31}P NMR of (dppe)NiCys. A series of aqueous 0.1 M phosphate buffers covering the pH range of 2−10 were prepared from potassium phosphates and phosphoric acid and calibrated using an Accumet model 20 (Fisher Scientific) pH meter. Solutions of (dppe)NiCys (4 mg in 2 mL) were prepared in the respective buffer, spectra were recorded, and the solutions were referenced to a sealed capillary filled with 1 M phosphoric acid as the internal standard.

X-ray Crystallography of [(dppe)NiCysAm]PF_6. An orange block crystal of [(dppe)NiCysAm]PF_6 measuring 0.35 × 0.35 × 0.30 mm was grown by slow evaporation of a methanol solution of the compound. A total of 14 307 unique reflections (10 230 with $I > 2\sigma$) were collected at 173(2) K temperature using a Rigaku AFC8 Mercury CCD diffractometer. The structure was solved by direct methods and expanded using Fourier techniques.[20] All non-hydrogen atoms were refined anisotropically. Hydrogen atoms were included as riding atoms but not refined. The standard deviation of an observation of the unit weight was calculated. All calculations were performed using the software *CrystalClear*[21] and *Crystal-Structure* (version 1.3.6) from Rigaku[22] and Crystals Issue 10 by Watkin et al.[23] except for refinement, which was performed using *SHELX-97*. Refinement parameters are summarized in Table 1. Selected bond distances and angles are presented in Table 2.

Results and Discussion

Both of the chelating phosphines used in this work yielded square-planar nickel−cysteine complexes. UV−vis electronic

(19) Han, R.; Looney, A.; McNeil, K.; Parkin, G.; Rheingold, A. L.; Haggerty, B. S. *J. Inorg. Biochem.* **1993**, *49*, 105−121.

(20) Beurskens, P. T.; Admiraal, G.; Beurskens, G.; Bosman, W. P.; de Gelder, R.; Israel, R.; Smits, M. M. *The DIRDIF-99 program system*; Technical Report of the Crystallography Laboratory, University of Nijmegen; University of Nijmegen: Nijmegen, The Netherlands, 1999.

(21) *Rigaku CrystalClear Software User's Guide*; Molecular Structure Corp.: The Woodlands, TX, 1999.

(22) *Rigaku and Rigaku/MSC*, 3.6.0 ed.; Molecular Structure Corp.: The Woodlands, TX, 2000−2004.

(23) Watkin, D. J.; Prout, C. K.; Carruthers, J. R.; Betteridge, P. W. *CRYSTALS Issue 10*; Chemical Crystallography Laboratory, University of Oxford, Oxford, U.K., 1996.

Table 1. Crystal, Collection, and Refinement Parameters for [(dppe)NiCysAm]PF_6

empirical formula	$C_{28}H_{30}F_6NNiP_3S$
fw	678.21
cryst size, mm^3	$0.42 \times 0.42 \times 0.35$
T, K	173(2)
wavelength, Å	0.710 70
cryst syst, space group	monoclinic, $P2_1/n$
unit cell dimens	
a, Å	19.919(6)
b, Å	13.482(4)
c, Å	22.577(7)
α, deg	90
β, deg	92.851(7)
γ, deg	90
V, $Å^3$	6056(3)
Z, density (calcd), g/cm^3	4, 1.49
abs coeff, mm^{-1}	0.925
$F(000)$	2784
θ range for data collection	1.82−28.00
limiting indices	$-25 \le h \le 26$, $-17 \le k \le 17$, $-29 \le l \le 20$
reflns colld/unique	56 029/14 307 [R(int) = 0.0722]
completeness to $\theta = 28.00$, %	97.7
max and min transmn	0.7378 and 0.6974
data/restraints/param	14 307/0/738
GOF on F^2	1.101
R, $R_w{}^a$ [$I > 2\sigma(I)$]	0.0756, 0.1744
R, $R_w{}^a$ (all reflns)	0.1063, 0.1994
largest diff peak and hole, $e/Å^3$	1.007 and −0.689

[a] $R = \sum[|(|F_o| - |F_c|)|]/\sum|F_o|$. $R_w = \{\sum[w(F_o^2 - F_c^2)^2]/\sum[w(F_o^2)^2]\}^{1/2}$. $w = 1/[\sigma^2(F_o^2) + (0.0709P)^2 + 9.5772P]$, where $P = (F_o^2 + 2F_c^2)/3$.

Table 2. Selected Bond Distances (Å) and Angles (deg) for (dppe)$NiCysAm^+$ Cations

cation 1		cation 2	
Ni(1)−N(1)	1.956(4)	Ni(2)−N(2)	1.948(4)
Ni(1)−S(1)	2.1663(13)	Ni(2)−S(2)	2.1591(14)
Ni(1)−P(1)	2.1518(13)	Ni(2)−P(3)	2.1406(14)
Ni(1)−P(2)	2.1663(13)	Ni(2)−P(4)	2.1719(14)
P(1)−Ni(1)−N(1)	173.12(15)	P(3)−Ni(2)−N(2)	167.49(14)
P(2)−Ni(1)−S(1)	165.71(5)	P(4)−Ni(2)−S(2)	166.80(5)
P(1)−Ni(1)−P(2)	86.50(5)	P(3)−Ni(2)−P(4)	87.60(5)
N(1)−Ni(1)−S(1)	89.46(13)	N(2)−Ni(2)−S(2)	89.94(13)
P(1)−Ni(1)−S(1)	90.20(5)	P(3)−Ni(2)−S(2)	89.41(5)
P(2)−Ni(1)−N(1)	95.46(13)	P(4)−Ni(2)−N(2)	95.73(13)

spectra were also consistent with those of square-planar P_2-NiSN coordination spheres for all complexes. Chelation of cysteine to nickel invariably required deprotonation of the thiol group prior to binding nickel. This S,N-donation was a constant theme and extended to experiments when the amino acid was anchored to heterogeneous supports. ^{31}P NMR spectra for the triphos system were complicated at room temperature by phosphorus-atom scrambling characteristic of this ligand; however, it was resolved at low temperature.

Crystal and Molecular Structure of [(dppe)NiCysAm]-PF_6. A square-planar geometry was confirmed for the (dppe)-$NiCysAm^+$ cation, consistent with low-spin nickel(II) centers and the diamagnetism demonstrated by NMR measurements for all of the phosphine−nickel−cysteine complexes. Two slightly different complex cations crystallized in the unit cell (one is shown in Figure 2); average bond distances from both cations are discussed below. These show slight differences in nickel−ligand bond distances and angles, as well as some differences in the rotation angles of the phosphine−phenyl substituents. One of the phenyl rings is rotated such that it is nearly coplanar with the P−Ni−S atom group (phosphorus trans to sulfur). The origin of this phenyl ring orientation must stem mostly from packing and steric effects because both (dppe)$NiCl_2$ and (dppe)$NiBr_2$ showed this same feature.[24a,25] Considerable twist angles (16−18°) were observed between planes defined by P−Ni−P and S−Ni−N atom groups, implying a departure from perfect square-planar coordination. Similar "T_d" twists have been observed in other square-planar nickel thiolates and (dppe)NiX_2 complexes.[26]

Different Ni−P distances were observed in (dppe)-$NiCysAm^+$ depending on whether the phosphorus was trans to nitrogen or sulfur. Somewhat shorter Ni−P distances were observed, average Ni−P = 2.146 Å, for the phosphorus trans to nitrogen compared to those trans to sulfur, average Ni−P = 2.169 Å. The shorter Ni−P distance trans to nitrogen and the longer Ni−P distance trans to sulfur in (dppe)$NiCysAm^+$ likely reflects a greater trans influence of sulfur over nitrogen (as suggested by reviewer 2). Despite this difference, the Ni−P distances in (dppe)$NiCysAm^+$ are comparable to values in other square-planar (dppe)Ni complexes.[27]

Ni−S distances in (dppe)$NiCysAm^+$, average Ni−S = 2.163 Å, are shorter than those in square-planar $Ni(Cys)_2{}^{2-}$, average Ni−S = 2.204 Å, in which the two sulfur atoms are in a trans configuration.[11b] Longer distances for the trans S−Ni−S arrangement in $Ni(Cys)_2{}^{2-}$ versus the trans P−Ni−S arrangement in (dppe)$NiCysAm^+$ likely result from more repulsive $S_{\pi\ donor}$−Ni−$S_{\pi\ donor}$ interactions coupled with additional thiolate−Ni−thiolate anionic repulsive forces. Such anionic repulsions are absent in (dppe)$NiCysAm^+$, and there is the added effect of a complementary $P_{\pi\ acceptor}$−Ni−$S_{\pi\ donor}$ interaction, both of which work to shorten the Ni−S bonds in these cations. This hypothesis is independently supported by a comparison to a longer average Ni−Cl distance in (dppe)$NiCl_2$, 2.200 Å,[24a] where comparable steric hindrance from phosphine−phenyl substituents is expected. The shorter Ni−S distance of (dppe)$NiCysAm^+$, despite a somewhat larger covalent radius for sulfur over chlorine, therefore implies strong Ni−S bonding in this cation.

Ni−N distances in (dppe)$NiCysAm^+$, average Ni−N = 1.951 Å, are longer than those in $Ni(Cys)_2{}^{2-}$, average Ni−N = 1.917 Å, and more similar to the distance in (bmedaco)-Ni, 1.940 Å, a square-planar complex with a *cis*-N_2NiS_2 coordination sphere [bmedaco = 1,5-bis(mercaptoethyl)-1,5-diazacyclooctane].[26a]

(24) (a) Busby, R.; Hursthouse, M. B.; Jarrett, P. S.; Lehmann, C. W.; Malik, K. M. A.; Phillips, C. *J. Chem. Soc., Dalton Trans.* **1993**, 3767−3770. (b) Jarrett, P. S.; Sadler, P. J. *Inorg. Chem.* **1991**, *30*, 2098−2104.

(25) Rahn, J. A.; Delian, A.; Nelson, J. H. *Inorg. Chem.* **1989**, *28*, 215−217.

(26) (a) Twist = 13.3° in (bmedaco)Ni: Smee, J. J.; Miller, M. L.; Grapperhaus, C. A.; Reibenspies, J. H.; Darensbourg, M. Y. *Inorg. Chem.* **2001**, *40*, 3601−3605. (b) Twist = 10−19° in (dppe)Ni(SPh′)$_2$: Autissier, V.; Clegg, W.; Harrington, R. W.; Henderson, R. A. *Inorg. Chem.* **2004**, *43*, 3098−3105. (c) Twist = 4° in (dppe)-$NiBr_2$: ref 25.

(27) Average Ni−P = 2.153 Å in (dppe)$NiCl_2$[24a] and 2.149 Å in (dppe)-$NiBr_2$.[25] Distances ranged from 2.158 to 2.189 Å in three different (dppe)Ni(SPh′).[26b]

Table 3. $^{31}P\{^1H\}$ NMR Results for Phosphine−Nickel−Cysteine Complexes

		δ P, ppm		
compound	solvent	trans to S	trans to N	other
[(dppe)NiCysEt]Cl	$CDCl_3$	59.8	52.1	
		J_{PP} = 48.3 Hz		
(dppe)NiCys−bead	$CDCl_3$	59.7	52.0	
		J_{PP} = 48.0 Hz		
(dppe)NiCys	CD_3OD	61.2	52.7	
		J_{PP} = 47.6 Hz		
[(dppe)NiCysAm]PF_6	$CDCl_3$	62.0	53.2	PF_6^-, −143.8, septet
		J_{PP} = 47.6 Hz		J_{PF} = 708 Hz
[(dppe)NiSeCysAm]Cl	$CDCl_3$	62.3	53.0	
		J_{PSe} = 54 Hz[c]	J_{PSe} = 40 Hz[c]	
		J_{PP} = 41 Hz		
[(triphos)NiCysEt]PF_6[a,b]				
trans	$(CD_3)_2CO$	17.8	6.7	−30.0, singlet[d]
		J_{PP} = 83 Hz		
cis		18.4	7.6	−32.6, singlet[d]
		J_{PP} = 86 Hz		
[(triphos)NiCysAm]PF_6[a,b]	$(CD_3)_2CO$	18.6	9.0	−31.1, singlet[d]
		J_{PP} = 83 Hz		
[(triphos)NiCysAm]PF_6 following aerial oxidation	$(CD_3)_2CO$	17.5	7.0	25.5, singlet, P═O[d]
		J_{PP} = 81 Hz		

[a] For comparison, (triphos)$NiCl_2$ in CH_2Cl_2 at −50 °C gives two broad singlets at +13 and −30 ppm, assigned as nickel-coordinated and free phosphine, based on respective 2:1 integration. [b] Recorded at −80 °C. [c] ^{77}Se, $I = 1/2$, 7.6%. [d] Uncoordinated $-PPh_2$ group. These samples also showed the characteristic septet of PF_6^- as is reported for [(dppe)NiCysAm]PF_6.

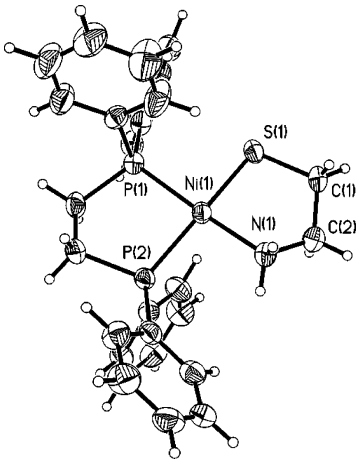

Figure 2. ORTEP diagram of the (dppe)NiCysAm$^+$ complex cation, one of two different cations in the unit cell. Ellipsoids are shown at the 50% probability level. The PF_6^- counterion is omitted for clarity.

UV−Vis Electronic Spectra Confirm That Square-Planar Coordination Persists in Solution. Room-temperature electronic spectra for all of the phosphine−nickel−cysteine complexes were consistent with those of square-planar P_2NiSN coordination spheres. This characteristic persisted even in common donor solvents like water and methanol. Square-planar nickel complexes typically have their lowest-energy d to d transition at wavelengths shorter than 600 nm, assigned as $^1A_{1g} \rightarrow {}^1A_{2g}$.[28] In general, this transition is blue-shifted when sulfur donors are replaced by nitrogen and phosphorus atoms. Accordingly, this transition appears near 634 nm in NiS_4 coordination spheres of Ni(detc)$_2$ and Ni(edt)$_2^{2-}$ (detc = diethyldithiocarbamate and edt = 1,2-ethanedithiolate),[29] near 550 and 457 nm in N_2S_2 coordination spheres of Ni(Cys−Gly−Cys)[8] and Ni(bmedach) [bmedach = *N*,*N*′-bis(2-mercaptoethyl)-1,4-diazacycloheptane],[26a] respectively, and at 502 nm for NiN_4 centers in Ni(L^8py_2)$^{2+}$ [L^8py_2 = 1,5-bis(2-pyridylmethyl)-1,5-diazacyclooctane].[30] The P_2NiSN geometries in the present complexes all show this transition near 495 nm. These d to d transitions (ϵ values range from 90 to 180 M^{-1} cm^{-1}) appear as shoulders against a second dominant transition near 380 nm assigned as a sulfur-to-nickel charge-transfer band based on ϵ values in the range from 730 to 1110 M^{-1} cm^{-1}.

^{1}H NMR Results for (dppe)NiCysEt$^+$ That Support P−Ni−S Long-Range Overlap. NMR (^1H, ^{13}C, and ^{31}P) measurements of (dppe)NiCysEt$^+$ indicated significant long-range coupling facilitated by the phosphorus−nickel−cysteine bonding network. A ^{13}C DEPT 135 experiment (Figure S1 in the Supporting Information) unambiguously identified the α-carbon resonance of the cysteine backbone at 64.1 ppm. An HMQC experiment (Figure S2 in the Supporting Information) indicated the single α-proton resonance at 4.35 ppm and the two different β protons at 3.35 and 2.79 ppm. There has to date been some variation on the assignment of α protons on cysteine ethyl ester chelated to nickel(II) and cobalt(III). The α-proton resonance of square-planar Ni(CysEt)$_2$ was assigned to 2.75 ppm,[11b] and for six-coordinate $Co^{III}(en)_2(CysEt)^+$, it was assigned to 4 ppm (en = ethylenediamine).[31] Both of the α- and β-carbon atoms of cysteine couple significantly to the phosphorus atoms of dppe, with J_{CP} in the proton-decoupled ^{13}C NMR spectrum of 9.1 and 11.3 Hz, respectively. The coupling constants are comparable to the two-bond J_{CP} values observed for the ethylene backbone of dppe (11.0 and 16.0 Hz). This through-

(28) Lever, A. B. P. *Inorganic Electronic Spectroscopy*; Elsevier: New York, 1968; p 344.
(29) (a) Cavell, K. J.; Magee, R. J.; Hill, J. O. *J. Inorg. Nucl. Chem.* **1979**, *41*, 1281. (b) Snyder, B. S.; Rao, Ch. P.; Holm, R. H. *Aust. J. Chem.* **1986**, *39*, 963−974.
(30) Fox, D. C.; Fiedler, A. T.; Halfen, H. L.; Brunold, T. C.; Halfen, J. A. *J. Am. Chem. Soc.* **2004**, *126*, 7627−7638.
(31) Sloan, C. P.; Krueger, J. H. *Inorg. Chem.* **1975**, *14*, 1481−1485.

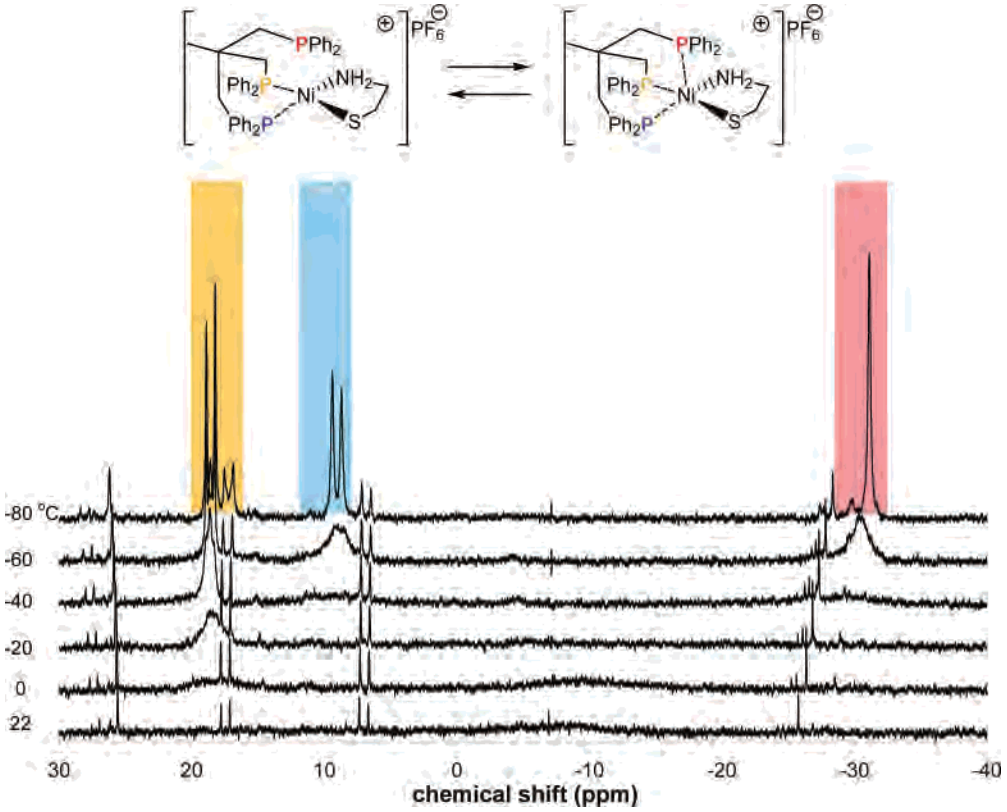

Figure 3. Temperature-dependent ^{31}P NMR spectra of [(triphos)NiCysAm]PF_6 in acetone-d_6. Sharp resonances apparent in the 22 °C range are assigned to adventitious oxidized material that does not participate in the proposed scrambling process. See Figure 4.

bond coupling indicates the influence of the nickel d orbital delocalization onto the cysteine backbone of the complex.

This through-bond coupling results from the strong trans influence of phosphorus and sulfur. Two additional NMR experiments support this conclusion. The selenium analogue of (dppe)$NiCysAm^+$ was prepared using selenocystamine and studied by ^{31}P NMR in order to assign each phosphorus signal to either the one trans to the chalcogen or the one trans to nitrogen. The only peaks in the spectrum of this sample were the two inequivalent ^{31}P NMR signals of (dppe)-$NiSeCysAm^+$ at 62.3 and 53.0 ppm (J_{PP} = 41 Hz). The similarity of this spectrum to the sulfur analogue, (dppe)-$NiCysAm^+$, recorded in the same protiomethanol medium, confirms the same essential P_2Ni(Se or S)N square-planar geometry for both complexes. At the base of each phosphorus doublet, there also appeared natural abundant ^{77}Se NMR multiplet satellites (I = $^1/_2$, 7.6%). The Se−P hyperfine splittings were inequivalent for the two phosphorus signals. The downfield 62.3 ppm resonance had J_{PSe} = 54 Hz, while the upfield 53.0 ppm resonance had J_{PSe} = 40 Hz. This larger J_{PSe} implies that the phosphorus atom assigned to the downfield resonance interacts more strongly with the chalcogen, a result of strong trans P−Ni−(S or Se) π interaction. The more downfield resonance is therefore assigned to the phosphorus trans to the chalcogen.

Temperature-Dependent Phosphorus Scrambling in (triphos)$NiCysAm^+$ and (triphos)$NiCysEt^+$. The strong trans P−Ni−S π overlap hinted at in (dppe)$NiCysEt^+$ was very evident in variable-temperature ^{31}P NMR spectra of fluxional (triphos)$NiCysAm^+$ and (triphos)$NiCysEt^+$ complexes (Figures 3 and 5). The fluxional behavior of triphos chelated to d^8 metals like nickel(II)[18,32] and platinum(II)[33] has been well-documented. Accordingly, the two distinct phosphorus resonances of square-planar (triphos)$NiCl_2$ were resolved in THF at −60 °C: −21.6 ppm (uncoordinated) and −22.6 ppm (coordinated) versus a chemical shift of −27.6 ppm for free triphos.[18] This same fluxional behavior was resolved for our own sample of (triphos)$NiCl_2$ in CH_2Cl_2 at −50 °C: 13 ppm (coordinated, integral = 2) and −30 ppm (uncoordinated, integral = 1). This fluxional behavior complicates air-free room-temperature spectra of (triphos)-$NiCysAm^+$ and (triphos)$NiCysEt^+$, but once resolved, the mechanism proposed to explain it (vide infra) supports the importance of P−Ni−S π bonding in these complexes.

Variable-temperature ^{31}P NMR spectra for [(triphos)-NiCysAm]PF_6 are summarized in Figure 3. At room temperature under nitrogen, the primary visible resonance in this sample is the sharp septet of the PF_6^- counterion at −144 ppm. A very broad coalesced resonance is also observable around −8 ppm. As this sample is cooled, resonances assignable to each of the three distinct phosphorus atoms of (triphos)$NiCysAm^+$ become apparent, and by −80 °C, these resonances are completely resolved with 1:1:1:1 integration relative to PF_6^-. Interestingly, the first resonance to emerge from the coalesced group is the most downfield resonance near 18 ppm (yellow highlight of Figure 3). This resonance

(32) (a) Bianchini, C.; Mealli, C.; Meli, A.; Scapacci, G. *Organometallics* **1983**, *2*, 141−143. (b) Bianchini, C.; Meli, A.; Orlandini, A.; Sacconi, L. *J. Organomet. Chem.* **1981**, *209*, 219−231.
(33) Colton, R.; Tedesco, V. *Inorg. Chim. Acta* **1992**, *202*, 95−100.

Scheme 1

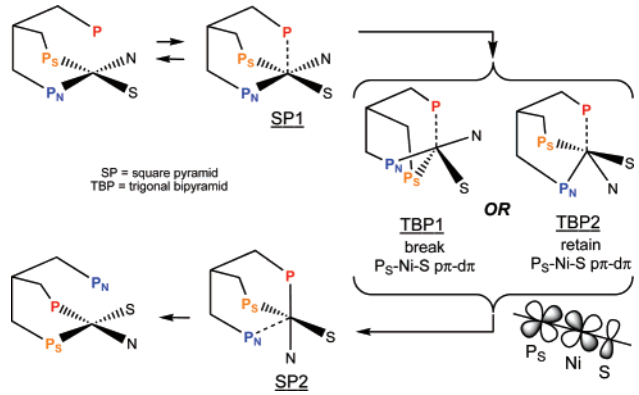

first becomes distinct at 0 °C; the remaining two resonances are not resolved until −40 °C, and all sharpen further with additional cooling. The most downfield and first-resolved resonance is assigned to a phosphorus atom that is impeded from participation in scrambling at temperatures as high as 0 °C, while the other two phosphorus atoms continue to scramble until they are cooled much further.

A mechanism for the scrambling of the three triphos phosphorus atoms is outlined in Scheme 1. This proposal invokes the common steps of Berry pseudorotation[34] that interconvert square-pyramidal (SP) and trigonal-bipyramidal (TBP) coordination spheres. A key assumption in this process is that the apical phosphorus (P of Scheme 1) binds to produce an initial SP intermediate. This seems more likely than a three-coordinate initial intermediate resulting from an alternative dissociative step, because an associative initial step is common for ligand substitution in square-planar systems.[35] Furthermore, reactions of the apical phosphorus (vide infra) and the lack of scrambling when bidentate phosphines are used, (dppe)NiCysR^{n+}, all support the proposed initial associative step described in Scheme 1. Berry pseudorotation then accounts for subsequent conversion of the SP intermediate into one of two possible secondary intermediates, TBP1 or TBP2.

Two different routes exist for the TBP intermediates to return to a square pyramid and regenerate a square-planar product. In Scheme 1, geometry SP1 can become TBP1, requiring disruption of the trans P_S−Ni−S π overlap, or SP1 can become TBP2, leading to a retention of this favorable π overlap. No similar trans π overlap is possible when the P_N−Ni−N angle is 180° (TBP1). TBP2 is therefore the preferred TBP geometry during the scrambling mechanism, keeping the P_S−Ni−S angle closer to 180°, so that SP2 is more likely to form. Ultimately, this mechanism explains the sluggishness of P_S to scramble with the apical P and further accounts for the continued rapid exchange of the apical P and P_N groups long after the resonance assigned to P_S has become well-resolved. The self-consistency of this explanation and peak assignments are supported by the resolved chemical shifts of (triphos)NiCysAm$^+$ (at −80 °C): uncoordinated P at −32 ppm (compared to −27 ppm for free triphos and to uncoordinated P in our (triphos)$NiCl_2$ sample), P_S at 18 ppm, and P_N at 9 ppm. Also, P_S is downfield-shifted and P_N is upfield-shifted from coordinated P_{Cl} in (triphos)$NiCl_2$, in agreement with changes seen when (dppe)NiCysR^{n+} are formed from (dppe)$NiCl_2$.

Oxidation of the uncoordinated phosphine group prevents its participation in the scrambling process of Scheme 1 and essentially locks the system into a square-planar geometry. Again, this supports the proposed initial associative step in Scheme 1. A similar result was observed in (triphos)Pt$(S_2)^+$, where S_2 represents chelating dithiocarbamates and dithiophosphites.[33] Like (triphos)$NiCl_2$, (triphos)Pt$(S_2)^+$ demonstrated temperature-dependent fluxional behavior so long as the apical phosphorus atom existed as a free phosphine. Reaction of (triphos)Pt$(S_2)^+$ with elemental sulfur led to the formation of (triphos/P═S)Pt$(S_2)^+$, where the free phosphine was converted to the phosphine sulfide. Clear room-temperature spectra were observed for (tripos/P═S)Pt$(S_2)^+$, consistent with that of square-planar platinum(II), chelated by two phosphorus atoms, and an uncoordinated P═S group.[33] Figure 4 demonstrates how aerial oxidation of (triphos)-NiCysAm$^+$ stops the fluxional behavior of this complex because the apical phosphine is converted to a phosphine oxide. Some oxidized (triphos)NiCysAm$^+$ is evident as an adventitious impurity in the room-temperature spectrum shown in Figures 3 and 4. At room temperature, therefore, (triphos/P═O)NiCysAm$^+$ gives a well-resolved spectrum (Figure 4) consistent with square-planar nickel(II).

The same basic splitting patterns and temperature-dependent fluxionality were also observed for (triphos)NiCysEt$^+$ (Figure 5), supporting the same nickel coordination geometry for this system. Here too, the resonance assigned to P_S is the first to become resolved at 0 °C, with eventual full resolution of all resonances by −80 °C in comparison to PF_6^- as an internal standard. Because of the chirality of the cysteine ethyl ester, (triphos)NiCysEt$^+$ exists in two diastereomers, labeled cis and trans in Figure 5. Steric hindrance should discourage the formation of the cis isomer because the bulky apical $-PPh_2$ group interacts with the $-CO_2Et$ ester functional group in the cis configuration. This hindrance is less in the trans isomer, and as a result, the trans form predominates at −80 °C (70% trans vs 30% cis) when all fluxionality is resolved.

pH Dependence of Cysteine Binding in (dppe)NiCys. An attempt was made to determine the ability of cysteine to accept protons when coordinated to nickel as (dppe)NiCys. In our experience, initial cysteine coordination to nickel(II) requires a cysteine thiolate formed by the addition of a base prior to introducing the metal ion. For this reason, we investigated the acid/base characteristics of nickel−cysteine after the complex had formed. Figure 6 summarizes the effect of variable pH on the ^{31}P NMR chemical shift of (dppe)-NiCys dissolved in aqueous phosphate buffers. These data indicate that two different processes are occurring in these mixtures. First, a monotonous downfield movement in the

(34) Casanova, D.; Cirera, J.; Llunell, M.; Alemany, P.; Avnir, D.; Alvarez, S. *J. Am. Chem. Soc.* **2004**, *126*, 1755−1763.
(35) (a) Casares, J. A.; Espinet, P.; Martínez-Ilarduya, J. M.; Mucientes, J. J.; Salas, G. *Inorg. Chem.* **2007**, *46*, 1027−1032. (b) Cooper, J.; Ziegler, T. *Inorg. Chem.* **2002**, *41*, 6614−6622. (c) Katakis, D.; Gordon, G. *Mechanisms of Inorganic Reactions*; Wiley-Interscience: New York, 1987; pp 191−195.

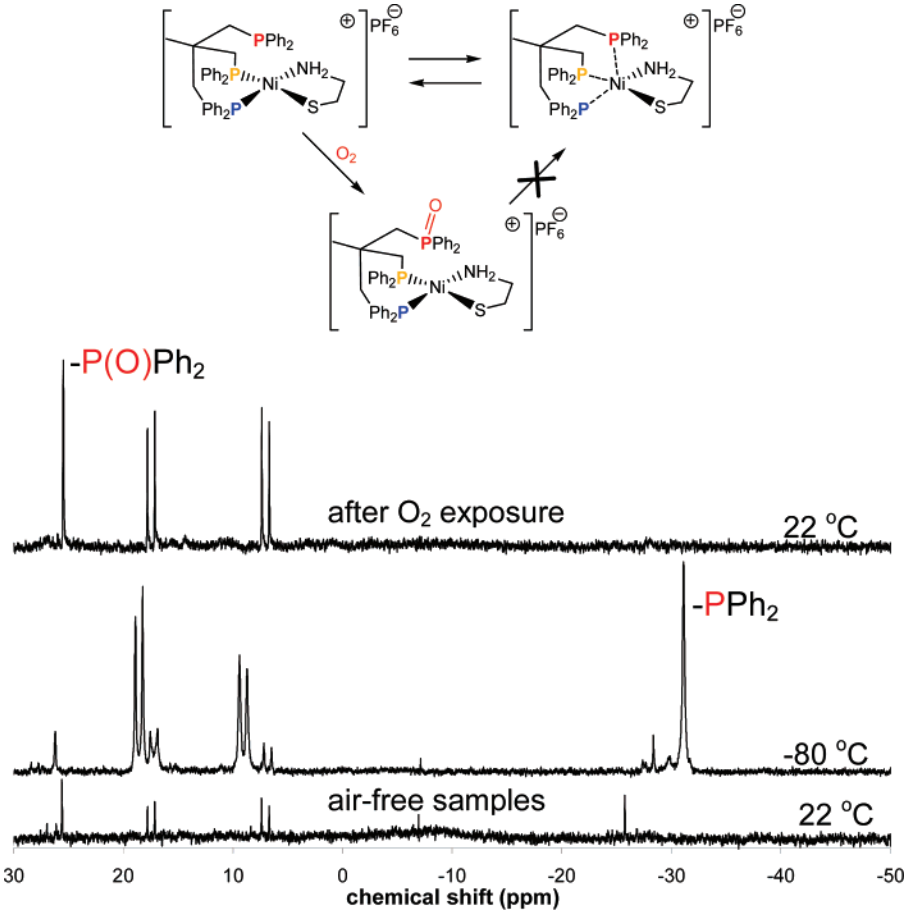

Figure 4. Effect of atmospheric oxidation on the ^{31}P NMR spectrum of [(triphos)NiCysAm]PF_6 in acetone-d_6. The bottom spectrum was recorded at room temperature under nitrogen. The middle spectrum was recorded at −80 °C under nitrogen, demonstrating resolution of each of the three distinct phosphorus signals. The top spectrum was recorded at room temperature after exhaustive aerial oxidation. All resonances in the −80 °C and oxidized spectra show 1:1 integration with the septet of PF_6^- that serves as an internal standard in these spectra.

phosphorus resonances is observed beginning at pH 6 and continuing to below pH 3. Significantly, even at quite low pH values, the characteristic doublets of (dppe)Ni(Cys)H$^+$ are dominant resonances in the spectrum.

A second reaction in this process is evident beginning at pH 4. At this and lower pH values, a singlet assignable to $(dppe)_2Ni^{+2}$ (δ = 56.3 ppm)[24b] begins to emerge and grow as still lower pH values are reached. The appearance of this product of (dppe)NiCys degradation implies that, at some point during the protonation process, a (dppe)Ni(Cys)H$^+$ species must exist, and because of its weakened donor strength toward nickel, this leads to cysteine loss and the eventual formation of $(dppe)_2Ni^{+2}$ by scavenging dppe from an adjacent metal center.

An initial protonation of cysteine dppeNiCys could occur at either the carboxylate or the coordinated thiolate group because of their available lone pairs; however, (dppe)-NiCysAm$^+$, which lacks the carboxylate group, showed no similar pH-dependent shifts. The change in the chemical shift with the pH suggests a pK_a of 3−4 for protonated (dppe)-NiCys. Free cysteine has respective functional group pK_a's of 10.8 (−NH_2), 8.3 (−SH), and 1.7 (−CO_2H) by comparison.[36] A 3.5 unit decrease in the thiol pK_a when coordinated to nickel was observed in *mer*-(triphos)NiS(H)Et^{2+} (from a pK_a of 10.6 in free HSEt to 7.1 in the phosphine complex).[17] A similar size decrease would be expected for cysteine thiol versus (dppe)NiCysH$^+$.[37] (dppe)NiCysAm$^+$ showed no similar pH-dependent shift, making the dangling carboxylate group the likely initial protonation site on (dppe)NiCys. A pK_a of 2.4 was measured for coordinated cysteine in six-coordinate $(en)_2Co^{III}Cys^+$, and this was assigned to the protonation of the uncoordinated carboxylate.[38] It is not surprising that cysteine loss was not reported in this system, where cobalt(III)−cysteine bonds will be much less labile than nickel(II)−cysteine. Similarly, bis(glycine dipeptide) complexes of nickel(III) underwent ligand loss from nickel, and an initial protonation at the dangling carboxylate was proposed.[39] Attempts to protonate any (dppe)NiCysR^{n+} with acids possessing a coordinating conjugate base all resulted in cysteine loss and the formation of the corresponding (dppe)Ni(base) complexes, confirmed by ^{31}P NMR [i.e., $(dppe)NiCl_2$ from HCl and $(dppe)Ni(O_2CCR_3)^+$ from HO_2CCH_3, HO_2CCF_3, and HO_2CCCl_3]. Similar acid-induced

(36) Stryer, L. *Biochemistry*, 4th ed.; W. H. Freeman and Co.: New York, 1995; p 23.

(37) Hightower, K. E.; Huang, C.-c.; Casey, P. J.; Fierke, C. A. *Biochemistry* **1998**, *37*, 15555−15562.

(38) Herting, D. L.; Sloan, C. P.; Cabral, A. W.; Krueger, J. H. *Inorg. Chem.* **1978**, *17*, 1649−1654.

(39) Jacobs, S. A.; Margerum, D. W. *Inorg. Chem.* **1984**, *23*, 1195−1201.

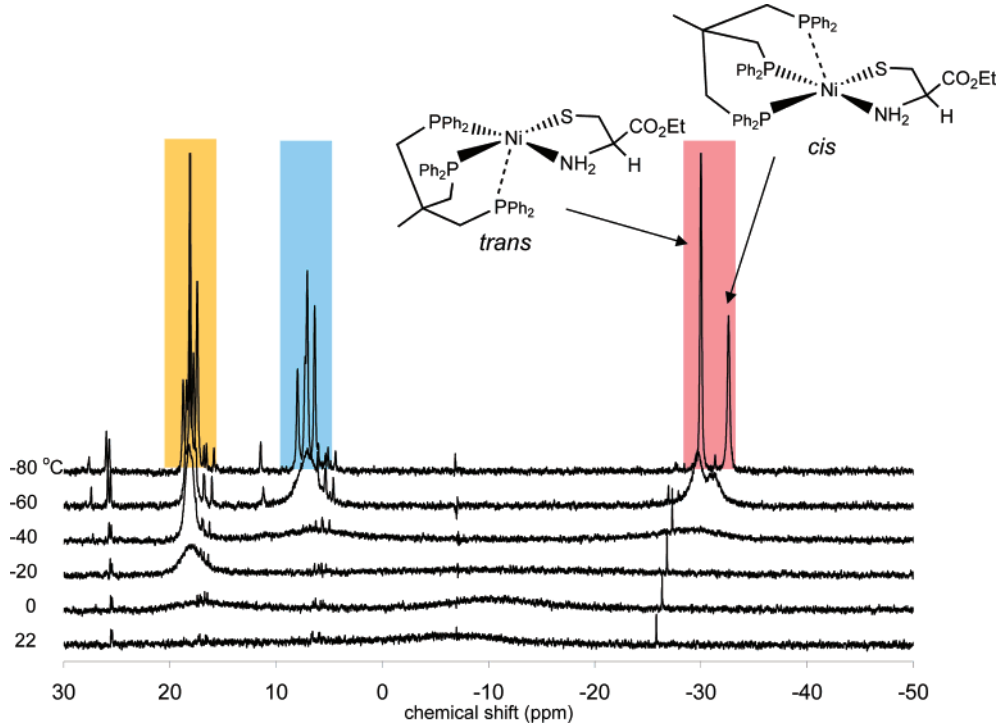

Figure 5. Temperature-dependent ^{31}P NMR spectra of [(triphos)NiCysEt]PF_6 in acetone-d_6. The two different diastereomers (based on L-cysteine) of the complex are indicated by the two different resonances assignable to the uncoordinated phosphorus atom. These singlets integrate to about 70% of the trans isomer and 30% of the cis isomer.

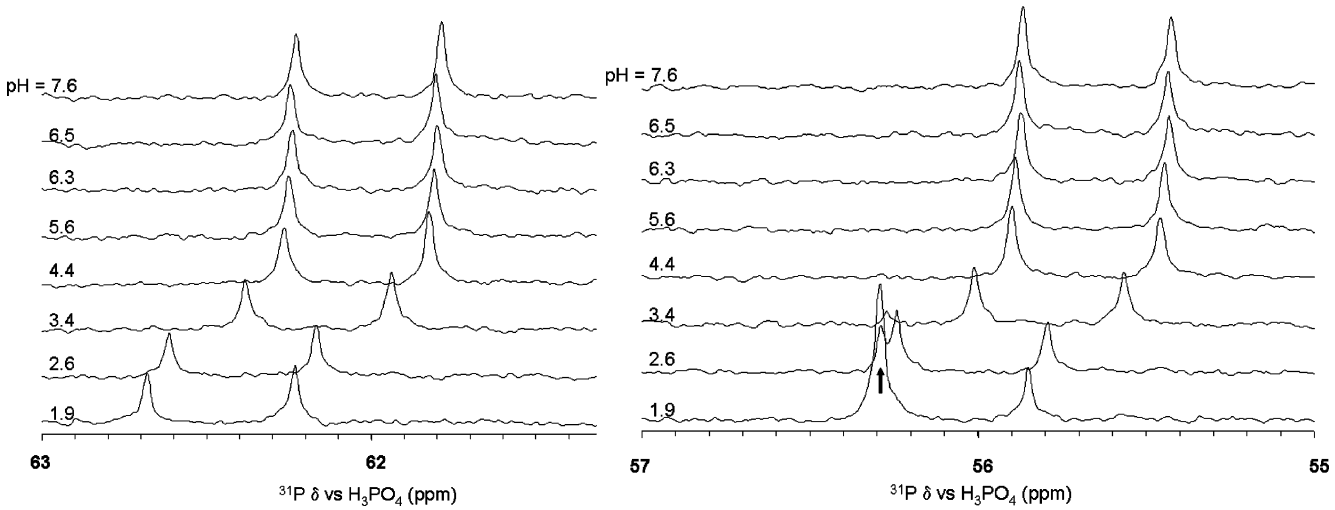

Figure 6. pH-dependent ^{31}P NMR spectra of (dppe)NiCys in 0.1 M aqueous phosphate buffers. Spectra are close-ups of the 63−61 and 57−55 ppm regions. The arrow near 56.3 ppm represents the singlet assigned to $(dppe)_2Ni^{2+}$ in the mixture. The heightened intensity is due to its coincidence with the downfield half of the $(dppe)NiCys(H)^+$ doublet.

thiolate losses were reported for $(dppe)Ni(SPh')_2$, where SPh′ respresents various para-substituted thiophenolates.[26b]

Protonation of the carboxylate in (dppe)NiCys does not initially lead to cysteine loss from nickel. Rather, a second intramolecular proton transfer to either sulfur or nitrogen coordinated to nickel must follow, causing eventual scission of cysteine from nickel. The amine group's proximity to the $-CO_2H$ group thus formed favors proton transfer to nitrogen; however, the Ni−N bond would have to first weaken or break to render the nitrogen lone pair more accessible to the proton. The thiolate group is still within reach of the $-CO_2H$ proton, and it should be possible to protonate one of the sulfur lone pairs while retaining a measure of nickel−cysteine integrity. Theoretical and experimental results on NiSOD active sites and related models suggest that shorter nickel−cysteine bonds result with sulfur protonation.[40] Large Ni−S force constants derived from NiSOD Raman measurements described the strength of the nickel−cysteine bonds in these systems, underscoring their stability if protonated.[41] Mass spectrometry confirmed the formation and integrity of (dppe)-$Ni(Cys)H^+$ in dispersed aerosols, where this was the primary positive ion observed (m/e = 576), including the correct

(40) Fiedler, A. T.; Bryngelson, P. A.; Maroney, M. J.; Brunold, T. C. *J. Am. Chem. Soc.* **2005**, *127*, 5449−5462.
(41) Fiedler, A. T.; Brunold, T. C. *Inorg. Chem.* **2007**, ASAP, Web Release Date: Feb 13, 2007.

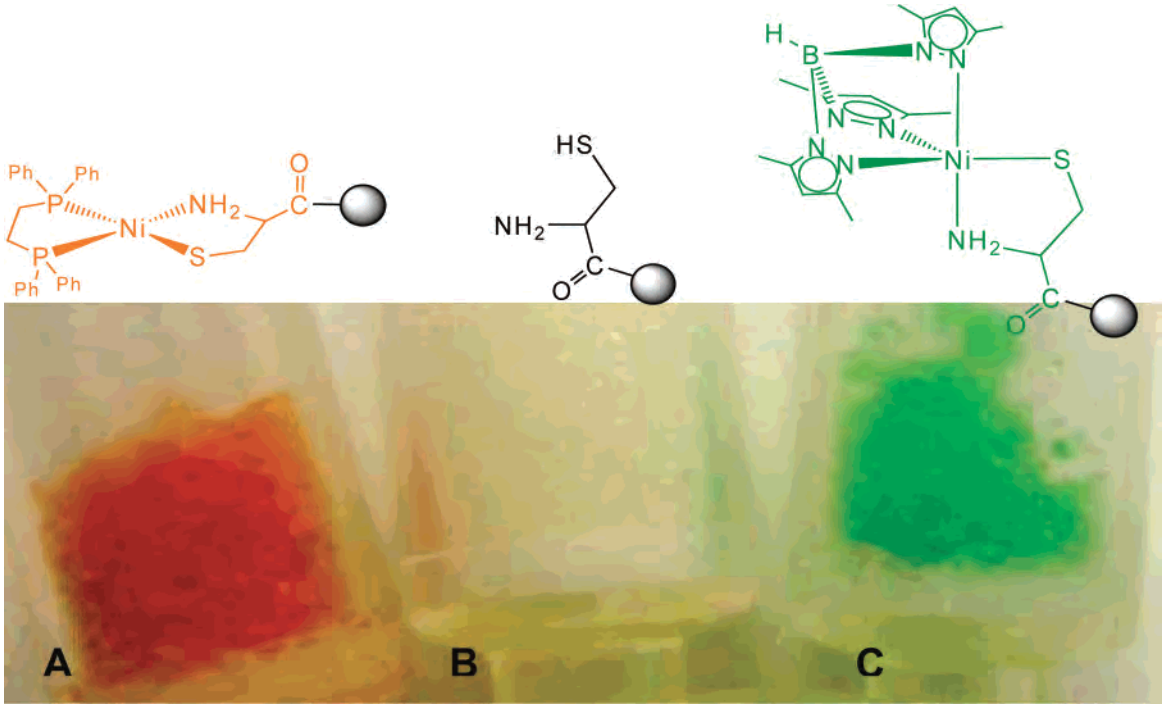

Figure 7. Brightly colored (dppe)Ni−Cys-bead (A) and Tp*Ni−Cys-bead complexes (C) formed from colorless bead-supported cysteine (B). The orange and green product beads have been thoroughly washed of residual reaction mixtures.

isotope distribution pattern. The more downfield ^{31}P NMR chemical shifts observed for (dppe)NiCysEt$^+$ and protonated (dppe)NiCys (also a monocation) are consistent with the trend observed in the pH-dependent spectra of (dppe)NiCys.

Hydrolysis of cysteine ethyl ester was observed in basic conditions. At pH 10 (0.1 M phosphate buffer), the resonances typical of (dppe)NiCysEt$^+$ abruptly shift to the higher values seen for (dppe)NiCys. Formation of (dppe)NiCys by this reaction was confirmed by a comparison of the spectrum of an original sample of (dppe)NiCys dissolved in the same basic medium. This reactivity is consistent with the established ability of nickel(II) to catalyze hydrolysis of carboxylic acid esters.[42]

Nickel(II) Preference for Cys over Met and Ser on Heterogeneous Supports. Nickel(II) ligated by dppe and Tp*$^-$ demonstrated a clear affinity for cysteine versus other amino acids when these amino acids were anchored to polystyrene synthesis beads. A series of amino acids (AA = Cys, Met, and Ser) anchored to Argogel beads were exposed to Tp*NiNO$_3$ in the presence of triethylamine (Figure 7). The originally colorless beads developed a green color when Cys was used, but they remained colorless for Met and Ser forms. This green color is consistent with the formation of a trigonal-bipyramidal Tp*NiCys-bead complex based on a comparison with the small-molecule complex, Tp*NiCysEt.[12] The reaction of red-orange (dppe)NiCl$_2$ with the same set of beads led to orange beads, indicative of the formation of (dppe)NiCys-bead (Figure 7).

The serine hydroxyl oxygen is a poor Lewis base[43] with nickel and the methyl thioether of Met-bead is a poorer donor than the anionic thiolate sulfur of cysteine.[44] Cysteine−nickel binding in the present systems requires free deprotonated sulfhydryl and amine groups. No binding of nickel to the AA-beads was observed without the addition of triethylamine. In this work, Fmoc-protected Cys-beads produced no discernible reaction with Tp*NiNO$_3$ or (dppe)NiCl$_2$ under inert atmospheres, when either the −SH or −NH$_2$ cysteine group was blocked by protecting groups.

Further proof of the coordinating role of the cysteine amine nitrogen came from reactions with a series of cysteine/glycine tripeptides in which the position of the cysteine was varied from the C-terminus internal position immediately adjacent to the bead tether (Gly−Gly−Cys-bead) to the N-terminus end of the tripeptide chain. The C-terminus side of the peptide forms an amide linkage with an amine pendant from the bead. The formation of colored beads was only observed for the variant with the Cys at the N-terminus of the tripeptide (Cys−Gly−Gly-bead). The need for N-terminus cysteine to coordinate nickel in these environments is in agreement with previous reports by Darensbourg's group.[9]

The color changes observed when Tp*NiNO$_3$ and (dppe)NiCl$_2$ were reacted with bead-bound cysteine were the same as those for homogeneous samples of (dppe)NiCysR^{n+} and Tp*NiCysR, but spectroscopic comparisons between the two forms were needed for definitive confirmation. ^{31}P NMR proved particularly useful in this regard; the only phosphorus resonances resulted from (dppe)Ni species, either in solution

(42) (a) Wells, M. A.; Bruice, T. C. *J. Am. Chem. Soc.* **1977**, *99*, 5341−5356. (b) Angelici, R. J.; Leach, B. E. *J. Am. Chem. Soc.* **1968**, *90*, 2499−2503. (c) Leach, B. E.; Angelici, R. J. *J. Am. Chem. Soc.* **1968**, *90*, 2504−2508.

(43) Rozema, D. B.; Poulter, C. D. *Biochemistry* **1999**, *38*, 13138−13146.

(44) Ochs, C.; Hahn, F. E.; Fröhlich, R. *Chem.−Eur. J.* **2000**, *6*, 2193−2199.

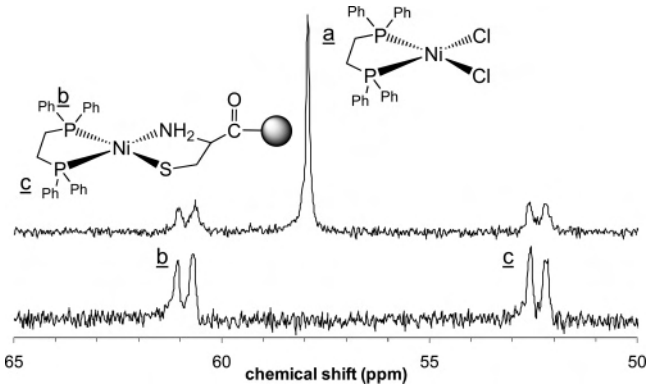

Figure 8. $^{31}P\{^1H\}$ NMR spectra of bead-supported (dppe)NiCys in $CDCl_3$. (Top) Reaction mixture of (dppe)Ni−Cys-bead and unreacted (dppe)$NiCl_2$. (Bottom) dppeNi−Cys-bead after washing to remove unreacted (dppe)-$NiCl_2$. These spectra were recorded for the orange bead sample pictured in Figure 7. Phosphorus assignments are indicated (a−c).

or bound to the bead (Figure 8). ^{31}P NMR spectra of the (dppe)NiCys-bead/(dppe)$NiCl_2$ slurry showed a resonance at 58.2 ppm due to unreacted (dppe)$NiCl_2$ in the bulk $CDCl_3$ solution. Two new resonances, each with $J_{PP} = 47$ Hz, were also observed at 61.1 and 52.5 ppm. After washing to remove unreacted starting material, the orange beads gave only the latter two doublets expected for (dppe)NiCys-bead. These are assigned to the two inequivalent phosphorus atoms of (dppe)NiCys-bead and are consistent with the independent small-molecule results described above.

Conclusions

The present results demonstrate strong dπ−pπ bonding involving sulfur, nickel, and the phosphorus atom trans to sulfur in square-planar nickel complexes. This interaction contributes to long-range dppe phosphorus coupling to the ethylene backbone of the coordinated cysteine. With the tridentate triphos ligand, this π interaction directs the rapid scrambling of the three phosphorus atoms via an associative initial step. In contrast, complementary experimental and theoretical work with Tp*Ni^+ has demonstrated the dominance of N−Ni σ interactions in this coordination sphere.[45] When dppe and pyrazolylborates (Tp^{R-}) or pyrazolylmethanes (Tm^R) are used simultaneously, low-spin $Ni^{II}P_2N_2$ coordination spheres result,[46] leading to κ^2 Tp^{R-} or Tm^R coordination. Bidentate Tp^{R-} leading to square-planar coordination is a more common characteristic of second- and third-row d^8 platinum metal ions.[47] For first-row nickel, this again demonstrates the commanding π overlap of phosphorus that tips the balance in favor of square-planar geometries.

The present results can be related to two properties in nickel enzymes: electron movement through nickel−cysteine manifolds and the stability of nickel−cysteinethiols. The nickel center of the carbon cluster in carbon monoxide dehydrogenase is known to be the site of CO coordination and oxidation, but electron paramagnetic resonance[3b] and L-edge X-ray absorption spectroscopy[48] measurements suggest that the electron density removed during this oxidation is not localized on nickel. Electron movement during CO oxidation could have them drawn from the Ni−CO unit onto the associated iron−cysteine framework of the carbon cluster, and the bonding manifold observed in the present phosphine−nickel−cysteine complexes suggests one route for this process. ENDOR measurements on [NiFe] hydrogenases detected the coupling of two different proton signals to nickel unpaired electron spin density. One signal was exchangeable with bulk protic media, and the other did not exchange.[49] The nonexchangeable proton coupling has been assigned to interaction with the β-methylene protons on the backbone of the coordinated cysteine ligand.[49,50] The strong J_{PC} between the phosphorus of dppe and the β-methylene of coordinated cysteine in (dppe)$NiCysEt^+$ points to a through-bond mechanism enhanced by Ni−S π bonding. A similar interaction has been observed by paramagnetic NMR in cobalt- and nickel-substituted rubredoxins[51] and could also contribute to the coupling of nickel spin density with the nonexchangeable β-methylene protons observed for [NiFe] hydrogenases.

Because cysteinethiol in (dppe)NiCys shows only limited integrity, postulated protonated Ni−S(H)Cys states for [NiFe] hydrogenase and for NiSOD groups must benefit from additional stabilizing influences. For both protein classes, the nickel−cysteine site possesses multiple cysteinyl thiolates coordinated to nickel. Multiple-sulfur coordination has been shown to improve the stability of metal thiols in protected protein environments[52] and in synthetic models.[53] Amide−nitrogen−nickel coordination, as seen in NiSOD groups, appears to offer no benefit for acid stability because bound peptides are still displaced by protonation in $Ni(Gly-Gly)_2$ that also possess amide−nitrogen−nickel bonds.[39] It is likely that the high dielectric aqueous environment used here encouraged cysteine displacement in (dppe)NiCys with protonation. Detailed pH-dependent stability studies of Ni-$(CysR)_n$ and $Ni(Cys-X_n-Cys)$ in variable dielectric media are warranted to outline the limits of nickel−cysteinethiol stability.

The water solubility and acid-induced lability of the phosphine−nickel−cysteine complexes encourage cytotoxicity studies for the (dppe)$NiCysR^{n+}$ class of compounds.

(45) Desrochers, P. J.; Telser, J.; Zvyagin, S. A.; Ozarowski, A.; Krzystek, J.; Vicic, D. A. *Inorg. Chem.* **2006**, *45*, 8930−8941.
(46) (a) $Tp^{PhMe}Ni(dppe)^+$: Uehara, K.; Hikichi, S.; Akita, M. *J. Chem. Soc., Dalton Trans.* **2002**, 3529−3538. Tp^{PhMe-} = hydrotris(3-phenyl-5-methylpyrazolyl)borate. (b) We independently prepared a sample of $[TmNi^{II}(dppe)](PF)_2$ as a bright-yellow solid and confirmed its diamagnetic square-planar geometry by ^{31}P NMR. Tm = tripyrazolylmethane. Phelan, A.; Thompson, L.; Linz, T.; Tarkka, R. 233rd ACS National Meeting, Chicago, IL, Mar 25−29, 2007, CHED 526.
(47) (a) Ruman, T.; Ciunik, Z.; Wolowiec, S. *Polyhedron* **2004**, *23*, 219−223. (b) Ruman, T.; Ciunik, Z.; Trzeciak, A. M.; Wolowiec, S.; Ziolkowski, J. J. *Organometallics* **2003**, *22*, 1072−1080. (c) Reinartz, S.; Baik, M.; White, P. S.; Brookhart, M.; Templeton, J. L. *Inorg. Chem.* **2001**, *40*, 4726−4732. (d) Chauby, V.; Le Berre, C. S.; Kalck, P.; Daran, J.-C.; Commenges, G. *Inorg. Chem.* **1996**, *35*, 6354−6355.
(48) Ralston, C. Y.; Wang, H.; Ragsdale, S. W.; Kumar, M.; Spangler, N. J.; Ludden, P. W.; Gu, W.; Jones, R. M.; Patil, D. S.; Cramer, S. P. *J. Am. Chem. Soc.* **2000**, *122*, 10553−10560.
(49) Brecht, M.; van Gastel, M.; Buhrke, T.; Friedrich, B.; Lubitz, W. *J. Am. Chem. Soc.* **2003**, *125*, 13075−13083.
(50) Whitehead, J. P.; Gurbiel, R. J.; Bagyinka, C.; Hoffman, B. M.; Maroney, M. J. *J. Am. Chem. Soc.* **1993**, *115*, 5629−5635.
(51) Moura, I.; Teixeira, M.; Moura, J. J. G.; LeGall, J. *J. Inorg. Biochem.* **1991**, *44*, 127−139.
(52) Dudev, T.; Lim, C. *J. Am. Chem. Soc.* **2002**, *124*, 6759−6766.
(53) Allan, C. B.; Davidson, G.; Choudhury, S. B.; Gu, Z.; Bose, K.; Day, R. O.; Maroney, M. J. *Inorg. Chem.* **1998**, *37*, 4166−4167.

Recently, labile $(dppe)_nCu^I$ complexes were shown to exhibit promising cytotoxicity,[54] motivated in part by the success of gold phosphines.[55] Targeted binding is a common strategy for metal-containing chemotherapeutic agents,[56] and coordinated cysteine has been investigated as a means of improving water solubility and biorecognition.[57] Some cancers demonstrate the ability to thrive at abnormally low pH levels, by inhibiting cell death normally triggered by intracellular acidification.[58] This more acidic tumor environment can help target anticancer therapies by exploiting pH-dependent reactivity.[59]

The observed selectivity of Tp^*Ni^+ for bead-supported N-terminus cysteine is a promising initial result for heterogeneous Tp^*Ni^+ work with amino acids and peptides. The reluctance of Tp^*Ni^+ to bind homocysteine thiolate and a readiness to bind cysteine thiolate[13] could be exploited, for example, as the basis for a colorimetric sensor for cysteine in the presence of homocysteine. Plasma homocysteine imbalance has been associated with a variety of pathologies.[60] Analytical detection of homocysteine versus cysteine often does not discriminate between these two major sulfur-containing amino acids,[61] so that selective homocysteine detection in plasma typically requires a cysteine separation step, prior to homocysteine detection.[62] Heterogeneous work involving Tp^*Ni^+ and more extensive cysteine peptides is ongoing, motivated by the present preliminary results.

Acknowledgment. Financial support was provided by the donors of the American Chemical Society Petroleum Research Fund (39644-B3 to P.J.D.), including a PRF SUMR Fellowship (to A.S.M.), and the University of Central Arkansas Research Council (to P.J.D.). R.M.T. is grateful to the BRIN program of the National Center for Research Resources of the National Institute of Health (Grant P20 RR-16460) for support. We recognize the assistance of Blake Richardson in helping to prepare some of the bead-bound peptide samples. Financial support was also provided by the National Science Foundation (Grant CCLI 0125711 to J.M.M. and R.M.T.) for the purchase of the NMR spectrometer.

Supporting Information Available: Complete listings of bond distances, angles, and atomic anisotropic thermal parameters for $[(dppe)NiCysAm]PF_6$, crystallographic data for this compound in CIF format, and DEPT 135 and HMQC NMR spectra with peak assignments for $[(dppe)NiCysEt]Cl$ in $CDCl_3$. This material is available free of charge via the Internet at http://pubs.acs.org.

IC701150Q

(54) Sanghamitra, N. J.; Phatak, P.; Das, S.; Samuelson, A. G.; Somasundaram, K. *J. Med. Chem.* **2005**, *48*, 977−985.
(55) McKeage, M. J.; Maharaj, L.; Berners-Price, S. J. *Coord. Chem. Rev.* **2002**, *232*, 127−135.
(56) (a) Platinum: Barnes, K. R.; Lippard, S. J. *Met. Ions Biol. Syst.* **2004**, *42*, 143−177. (b) Titanium: Caruso, F.; Rossi, M. *Mini-Rev. Med. Chem.* **2004**, *4*, 49−60. (c) Gold: Mohamed, A. A.; Chen, J.; Bruce, A. E.; Bruce, M. R.; Krause-Bauer, J. A.; Hill, D. T. *Inorg. Chem.* **2003**, *42*, 2203−2205.
(57) Waern, J. B.; Harding, M. M. *Inorg. Chem.* **2004**, *43*, 206−213.
(58) (a) Runge, S. W.; Haley, U. B. *Recent Res. Dev. Cell. Biochem.* **2003**, *1*, 177−192. (b) Boyle, K. M.; Irwin, J. P.; Humes, B. R.; Runge, S. W. *J. Cell Biochem.* **1997**, *67*, 231−240. (c) Schornack, P. A.; Gillies, R. J. *Neoplasia* **2003**, *5*, 135−145.
(59) Mahoney, B. P.; Raghunand, N.; Baggett, B.; Gillies, R. J. *Biochem. Pharmacol.* **2003**, *66*, 1207−1218.
(60) (a) Vitamin B_{12} deficiencies: Stangl, G. I.; Roth-Maier, D. A.; Kirchgessner, M. *J. Nutr.* **2000**, *130*, 3038−3044. (b) Vacular diseases: Marouf, R.; Zubaid, M.; Mojiminiyi, O. A.; Qurtom, M.; Abdella, N. A.; Al Wazzan, H.; Al Humood, S. *South. Med. J.* **2006**, *99*, 811−816. (c) Renal failure: Baber, U.; Toto, R. D.; de Lemos, J. A. *Am. Heart J.* **2007**, *153*, 471−477. Urquhart, B. L.; Freeman, D. J.; Spence, J. D.; House, A. A. *Am. J. Kidney Dis.* **2007**, *49*, 109−117.
(61) Rusin, O.; St. Luce, N. N.; Agbaria, R. A.; Escobedo, J. O.; Jiang, S.; Warner, I. M.; Dawan, F. B.; Lian, K.; Strongin, R. M. *J. Am. Chem. Soc.* **2004**, *126*, 438−439.
(62) Nekrassova, O.; Lawrence, N. S.; Compton, R. G. *Talanta* **2003**, *60*, 1085−1095.